Dalton Transactions

ROYAL SOCIETY OF CHEMISTRY

PAPER

View Article Online
View Journal

Published on 27 October 2021. Downloaded by University of Louisville on 11/18/2021 3:18:04 PM.

Check for updates

Cite this: DOI: 10.1039/d1dt02136b

Metal triflate formation of C_{12}–C_{22} phenolic compounds by the simultaneous C–O breaking and C–C coupling of benzyl phenyl ether†

Mohammad Shahinur Rahaman, [a] Sarttrawut Tulaphol, [b] Ashten Molley,[a] Kyle Mills,[a] Md. Anwar Hossain, [a] Daniel Yelle, [c] Thana Maihom [d] and Noppadon Sathitsuksanoh *[a]

Received 27th June 2021,
Accepted 25th October 2021

DOI: 10.1039/d1dt02136b

rsc.li/dalton

Catalytic pathways to produce high carbon number compounds from benzyl phenyl ether require multiple steps to break the aryl etheric carbon–oxygen bonds; these steps are followed by energy-intensive processes to remove oxygen atoms and/or carbon–carbon coupling. Here, we show an upgrading strategy to transform benzyl phenyl ether into large phenolic (C_{12}–C_{22}) compounds by a one-step C–O breaking and C–C coupling catalyzed by metal triflates under a mild condition (100 °C and 1 bar). Hafnium triflate was the most selective for the desired products. In addition, we measured the effect of solvent polarity on the catalytic performance. Solvents with a polarity index of less than 3.4 promoted the catalytic activity and selectivity to C_{12}–C_{22} phenolic products. These C_{12}–C_{22} phenolic compounds have potential applications for phenol–formaldehyde polymers, diesel/jet fuels, and liquid organic hydrogen carriers.

Introduction

The development of chemical conversion strategies for lignin is important for the production of fuels and chemicals from renewable plant lignocellulose.[1,2] Lignin may account for as much as 35 wt% of the total lignocellulosic biomass. Lignin is a highly branched polymer composed of hydroxy- and methoxy-substituted phenylpropane (C_3C_6) units joined by carbon–carbon (C–C) and ether (C–O) linkages. The C–O linkages are abundant in lignin, including β-O-4, α-O-4, and 4-O-5.[3–5] The relative ratio of these linkages in lignin depends on the plant species (Table S1†). In general, most current lignin conversion strategies start from depolymerization (hydrolysis or pyrolysis) to produce lignin fragments, *i.e.*, C_6–C_9 phenolic compounds.[6,7] Then, the phenolic compounds undergo hydrodeoxygenation and/or hydrogenation to produce C_6–C_9 hydrocarbons, suitable for gasoline.

Although low carbon number phenolic compounds are readily obtainable from lignin, the use of lignin biomass would be greatly stimulated by the availability of an efficient route to transform lignin into higher carbon phenolic compounds (C_{12}–C_{22}) as precursors for diesel- and jet-range fuels.[7,8] We can increase the carbon number *via* C–C coupling reactions with lignin-derived monomers.[8] For example, Zhang *et al.*[9] and Bi *et al.*[10] performed a cascade of pyrolysis of sawdust/lignin into low-carbon phenolics, followed by the alkylation of these low-carbon phenolics by the ionic liquid $[C_4C_1im]Cl$–$2AlCl_3$ (1-butyl-3-methylimidazolium chloroaluminate) into C_8–C_{15} phenolics. The combined C–C coupling and hydrodeoxygenation of phenol and substituted phenols to yield bi-cycloalkanes (*i.e.*, C_{12}–C_{18}) can be achieved using a cascade reaction over Pd nanoparticles on acidic support at 200 °C and 50 bar H_2.[11] These approaches are effective, but there are two major impediments to the transformation of lignin and its fragments to C_{12}–C_{22} phenolic compounds: (1) severe depolymerization conditions[12] because of the high stability of the aryl etheric C–O bonds,[13,14] and (2) multiple reaction steps (C–O breaking and C–C coupling) required to produce larger chemical precursors (C_{12}–C_{22} phenolic compounds),[8] as depicted in Scheme 1. These challenges contribute to the production cost and retard the adoption of developed technology.

Here, we describe a direct transformation of benzyl phenyl ether by simultaneous C–O bond breaking and C–C coupling catalyzed by metal triflates in a liquid phase reaction. Hafnium triflate was the most active and selective catalyst to produce desired C_{12}–C_{22} phenolic products in solvents with a polarity index lower than 3.4. Our findings establish a new, more efficient upgrading route for lignin model compounds.

[a]*Department of Chemical Engineering, University of Louisville, Louisville, KY 40292, USA. E-mail: N.sathitsuksanoh@louisville.edu*
[b]*Sustainable Polymer & Innovative Composite Materials Research Group, Department of Chemistry, Faculty of Science, King Mongkut's University of Technology Thonburi, Bangkok 10140, Thailand*
[c]*USDA, Forest Products Laboratory, Madison, WI, 53726, USA*
[d]*Department of Chemistry, Faculty of Liberal Arts and Science, Kasetsart University, Kamphaeng Saen Campus, Nakhon Pathom 73140, Thailand*
†Electronic supplementary information (ESI) available. See DOI: 10.1039/d1dt02136b

Published on 27 October 2021. Downloaded by University of Louisville on 11/18/2021 3:18:04 PM.

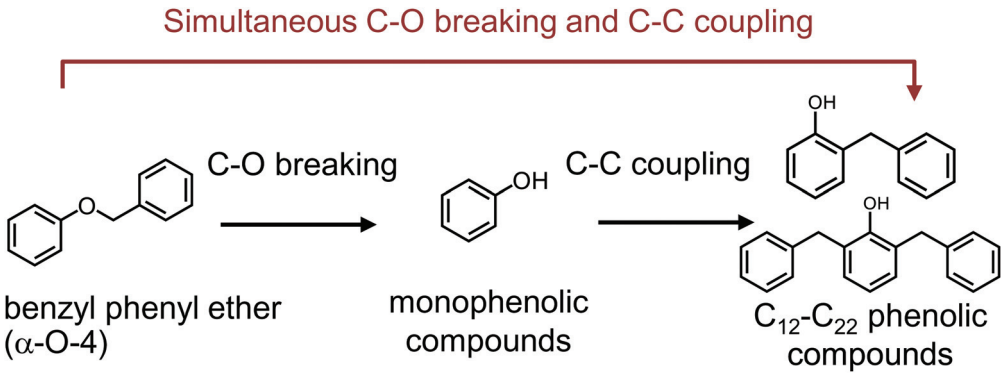

Scheme 1 Transformation pathways for benzyl phenyl ether (α-O-4) into C_{12}–C_{22} phenolic compounds.

Materials and methods

Materials

Benzyl phenyl ether (98 wt%, Sigma-Aldrich, St Louis, MO, USA), 2-phenethyl phenyl ether (99 wt%, Frinton Laboratories, Inc., Hainesport, NJ, USA), and diphenyl ether (99 wt%, Sigma-Aldrich) were used as received unless noted otherwise. *n*-Heptane (99 wt%, Beantown Chemical) and *n*-dodecane (≥99 wt%, Beantown Chemical) were used as a solvent and the internal standard, respectively, unless noted otherwise. Metal triflates, $La(OTf)_3$, $Al(OTf)_3$, $Ti(OTf)_4$, $Zn(OTf)_2$, $Yb(OTf)_3$, $Y(OTf)_3$, $Er(OTf)_3$, $Sc(OTf)_3$, $Fe(OTf)_3$, and $Hf(OTf)_4$, were purchased from a commercial supplier and used as received unless noted otherwise. These anhydrous metal triflates were stored in desiccators. All chemicals were used as received unless otherwise noted. Their CAS numbers, purity, and manufacturers are listed in Table S2.†

Catalysis testing

Reactions were conducted with solutions of benzyl phenyl ether in *n*-heptane and *n*-dodecane with a ratio of feed: *n*-heptane : dodecane = 1.0 : 8.5 : 0.5 by weight. Heptane was used as the reaction solvent; dodecane was added as the internal standard for quantifying conversion and product yields. The catalyst was 20 mol% of metal with respect to the benzyl phenyl ether feed. The catalysts were loaded in a glove box to minimize the effect of moisture on the activity of the metal triflates. The reaction mixture was stirred at 100 °C in a pressure vessel (Ace Glass Inc., Vineland, NJ, USA) containing a small magnetic stir bar and sealed using a polytetrafluoroethylene/silicone septa and metal crimp top. The sealed reactor was placed in a temperature-controlled silicon oil bath on a magnetic stir plate, and samples were taken at various times. The products were analyzed by Agilent gas chromatography (GC) (model 7890A, Agilent Technologies, Santa Clara, CA, USA) equipped with a DB-1701 column (Agilent Technologies, 30 m × 0.25 mm id, 0.25 μm). The GC parameters were the following: injection temperature was 275 °C, the FID detector temperature was 300 °C and the split ratio 1 : 50. The temperature program started at 50 °C and was held for 5 min; then, the temperature was increased at 10 °C min^{-1} to 200 °C, followed by a 10 min hold. Product separation and identification were performed by Agilent GC equipped with mass spectrometry (model 5977A, Agilent Technologies). The conversion of the feed and the product yields were calculated on a molar basis of carbon.

Theoretical details

All calculations were performed using the Gaussian 09 software[15] with M06-2X density functional and the def2TZVP basis set. We chose the M06-2X method because it was suggested for broad applications on main-group thermochemistry, kinetics, and noncovalent interactions.[16] All structural optimizations were fully relaxed. Vibrational frequency calculations were performed at the same level of theory to classify the nature of the stationary point as a minimum structure and gained the thermodynamic properties at 25 °C and 1 bar. To include the contributions from the solvent in the reaction enthalpies (ΔH^{rxn}) and free energies (ΔG^{rxn}), the polarizable continuum model[17] was performed.

Results

Screening of metal triflates for the conversion of benzyl phenyl ether

To determine the best-performing catalyst for the conversion of benzyl phenyl ether (α-O-4 linkage), compound **A**, we screened 10 metal triflates ($La(OTf)_3$, $Al(OTf)_3$, $Ti(OTf)_4$, $Zn(OTf)_2$, $Yb(OTf)_3$, $Y(OTf)_3$, $Er(OTf)_3$, $Sc(OTf)_3$, $Fe(OTf)_3$, and $Hf(OTf)_4$) at 100 °C and 1 bar (Fig. 1). At a given reaction condition (*i.e.*, 20 mol% of catalyst, 100 °C, 1 bar, and 1 h), $Hf(OTf)_4$ and $Fe(OTf)_3$ exhibited the highest activity with a complete conversion after 1 h. The reaction products consisted of three main compounds, (i) *o*- and *p*-benzylphenols (C_{13}, compound **B**); (ii) di-benzylphenols (C_{20}, compound **C**); and (iii) phenol (C_6, compound **D**). These two triflates at 20 mol% catalyst loading after 1 h showed 82–89% yield of desired products, *o*- and *p*-benzylphenols (**B**) and di-benzylphenols (**C**). Next, we decreased the loading of $Hf(OTf)_4$ and $Fe(OTf)_3$ to 2 mol% and performed the same reaction at 100 °C for 1 h. Interestingly,

This journal is © The Royal Society of Chemistry 2021

Published on 27 October 2021. Downloaded by University of Louisville on 11/18/2021 3:18:04 PM.

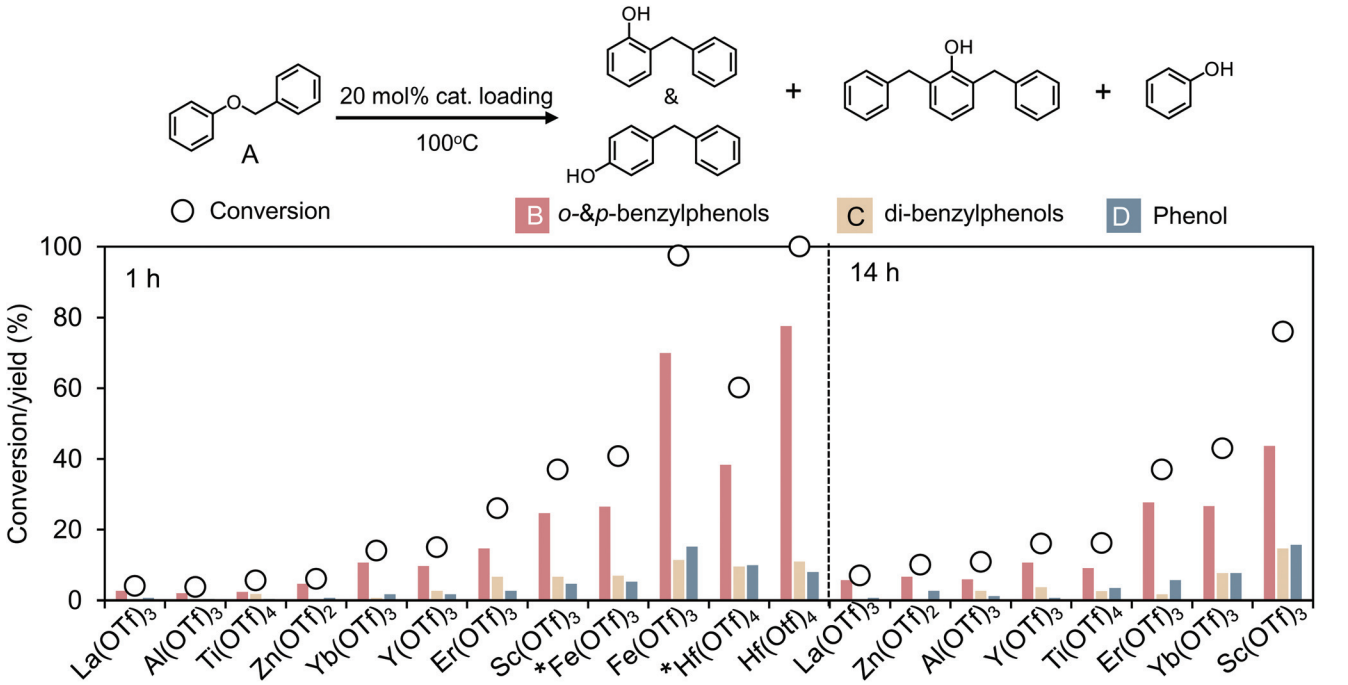

Fig. 1 Evaluation of metal triflate catalysts for the conversion of benzyl phenyl ether (A) and product yields (*o*- and *p*-benzylphenols (B), di-benzylphenols (C), and phenol (D)). Reaction conditions: feed = 0.26 mmol benzyl phenyl ether, feed/heptane/dodecane (internal standard) = 1.0 : 8.5 : 0.5 by weight, catalyst = 20 mol%, 100 °C, 1 bar, * catalyst = 2 mol%. Fig. S1† shows the representative gas chromatogram of the reaction products and their mass spectra.

we achieved 49% yield of desired products at 60% feed conversion under a low $Hf(OTf)_4$ loading, whereas $Fe(OTf)_3$ had 34% yield of the desired products and a lower conversion (41%) compared with $Hf(OTf)_4$ at a 2 mol% catalyst loading. The other eight metal triflates promoted significantly lower yields of the desired products at low conversions (below 40%) at 20 mol% catalyst. However, for all the experiments after 1 h, the selectivity towards **B** and **C** exceeded 75% regardless of the percent conversion (Table S3†). Further, we performed the same reaction using 20 mol% of these eight metal triflates with a longer reaction time of 14 h. We observed an increase in the feed conversion and yield towards desired products compared to those at 1 h. Although all metal triflates demonstrated an enhanced feed conversion and yield of the desired products at a prolonged reaction time (14 h) and 20 mol% catalyst loading, $Hf(OTf)_4$ had the highest conversion rate and yields of the desired product at a low catalyst loading (2 mol%). These results suggested that $Hf(OTf)_4$ was the most active and selective towards C_{12}–C_{22} phenolic compounds. Thus, we used $Hf(OTf)_4$ for the rest of the studies.

Effect of the chemical structure of C–O model compounds on catalytic performance

To understand the effect of the chemical structure of C–O model compounds on this chemical pathway, we conducted the same experiment in which we used the $Hf(OTf)_4$ catalyst but with two other model compounds, 2-phenethyl phenyl ether (compound **M** with β-O-4 linkage) and diphenyl ether (compound **N** with 4-O-5 linkage) (Fig. 2). Interestingly, $Hf(OTf)_4$ was essentially inactive in converting 2-phenethyl phenyl ether and diphenyl ether and showed <5% conversion.

The C–O bond cleavage of 2-phenethyl phenyl ether and diphenyl ether catalyzed by Ni[18,19] typically yields phenol and toluene as major products. However, we did not observe reaction products from the conversion of 2-phenethyl phenyl ether and diphenyl ether by $Hf(OTf)_4$. Huang *et al.* used $Yb(OTf)_3$ and more severe reaction conditions (200 °C, 4 h in methanol and 30 bar H_2) to convert phenethyl phenyl ether; they did not observe any conversion. Yang *et al.* used $In(OTf)_3$ with diphenyl ether at 330 °C for 1 h and observed 11% conversion.[20] The bond dissociation energies (BDE) of the C–O bond of diphenyl ether (4-O-5) and 2-phenethyl phenyl ether (β-O-4) are ~77 and 57 kcal mol^{-1}, respectively, greater than the BDE of benzyl phenyl ether (α-O-4, 49 kcal mol^{-1}).[21] Table S1† shows the relative lignin linkage content of softwood, hardwood, and grass and their BDEs. We did not observe the feed conversion under our reaction condition because a higher reaction temperature is required to cleave the C–O bond of these two model compounds. However, the formation of benzylphenols and di-benzylphenols from benzyl phenyl ether by metal triflates did not proceed by the hydrolysis of the C–O cleavage.

Energetics and proposed mechanism of benzyl phenyl ether transformation

On the basis of the resulting products, we proposed the chemical pathway shown in Fig. 3.

Published on 27 October 2021. Downloaded by University of Louisville on 11/18/2021 3:18:04 PM.

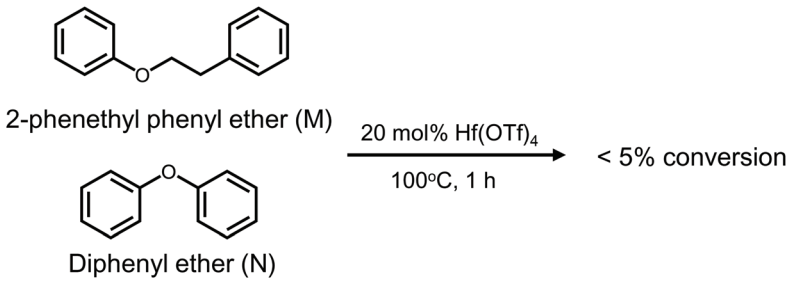

Fig. 2 Conversion of 2-phenethyl phenyl ether and diphenyl ether by $Hf(OTf)_4$. Reaction conditions: feed = 0.26 mmol 2-phenethyl phenyl ether or diphenyl ether, feed/heptane/dodecane (internal standard) = 1.0 : 8.5 : 0.5 by weight, $Hf(OTf)_4$ = 20 mol%, 100 °C, 1 bar, 1 h.

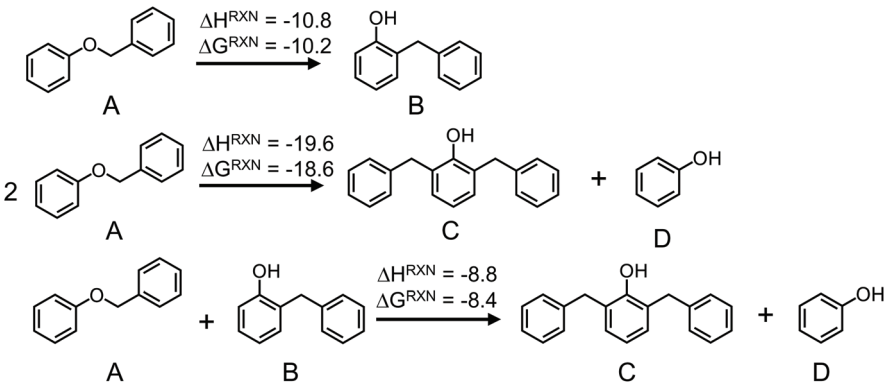

Fig. 3 Computed energetics of possible benzyl phenyl ether reactions at the M06-2X density functional and the def2TZVP basis set at 25 °C and 1 bar using heptane solvent. Note that energies are in kcal mol^{-1}. Coordinates of these species are shown in the ESI.

To validate the feasibility of the cleavage of the C–O bonds of benzyl phenyl ether and the formation of multi-ring precursors by C–C coupling, we determined the energetics using the M06-2X density functional and the def2TZVP basis set for the uncatalyzed reactions. These calculations suggested that the C–O breaking and C–C coupling reactions were thermodynamically favorable (*i.e.*, $\Delta G^{rxn} = -18.6$ to -8.4 kcal mol^{-1}) and exothermic (*i.e.*, $\Delta H^{rxn} = -19.6$ to -8.8 kcal mol^{-1}) for all possible reactions.

We proposed this mechanism based on relevant intermediates and products (Scheme 2). The strong Lewis acid from the metal center of metal triflates interacts with etheric oxygen (Lewis base) to form an O–aryl complexation (complex **E**).[22] As a result, the ether bond is polarized and heterolytically cleaved into a phenolated ion (intermediate **F**). Then, the charge stabilization within the resonance structure of **F** leads to the formation of a carbanion (intermediate **G**) that has a negative charge at a carbon atom on the ring.[23] For the C–C coupling step, we suggest that the carbanion (**G**) reacts with complex **E** *via* an electrophilic attack-type mechanism to form a keto-intermediate (**H**), which is eventually tautomerized into a more stable enol-compound (benzylphenols, **B**).

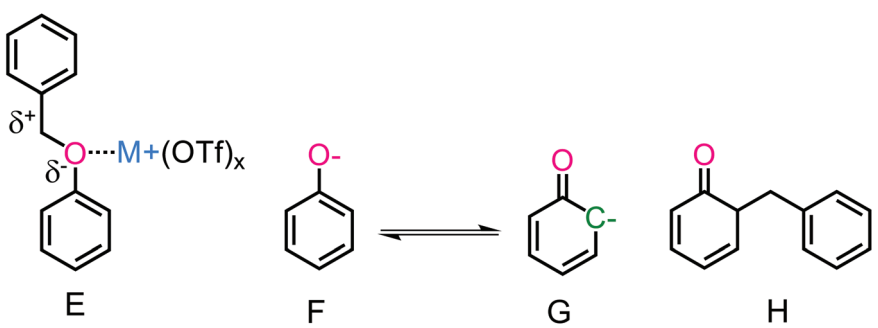

Scheme 2 The relevant intermediates in the proposed mechanism of the simultaneous C–O breaking and C–C coupling of benzyl phenyl ether.

 This journal is © The Royal Society of Chemistry 2021

Published on 27 October 2021. Downloaded by University of Louisville on 11/18/2021 3:18:04 PM.

In contrast, Yoon *et al.*[7] used silica–alumina to catalyze the conversion of benzyl phenyl ether into benzylphenols at 100 °C and 5 bar helium. However, the mechanism of the formation of benzylphenols by Brønsted acid sites was unknown. Therefore, the investigators proposed that the Brønsted acid sites of silica–alumina activated the C–O cleavage and catalyzed the Claisen rearrangement to produce benzylphenols. Further investigations in conjunction with the quantum calculations are needed to confirm the chemical pathway for the formation of benzylphenols.

Effect of solvents on the product selectivity of benzyl phenyl ether transformation

The solvent affects catalyst activity and product selectivity. To determine the effect of solvent polarity on the catalytic activity and product selectivity by $Hf(OTf)_4$, we varied the reaction solvents with polarity indexes from 0.0 to 6.6 (Table S4†). Feed conversion by $Hf(OTf)_4$ demonstrated a strong dependence on the solvent polarity (Fig. 4A). Relatively non-polar solvents (*i.e.*, *n*-heptane, *n*-octane, toluene, and DCM) were active (100% conversion) and yielded >68% of the desired products, *o*- and *p*-benzylphenols (**B**) and di-benzylphenols (**C**) (Fig. 4B). Interestingly, $Hf(OTf)_4$ became significantly less active (<31% conversion) in solvents with a polarity index greater than 3.4.

Discussion

Severe depolymerization and multiple transformation steps are the major challenges in upgrading lignin fragments.[8,12–14] Here, we described the conversion of benzyl phenyl ether into C_{12}–C_{22} phenolic compounds by metal triflates. Hafnium triflate, $Hf(OTf)_4$, was the most active in solvents with a polarity index of <3.4 and the most selective for C_{12}–C_{22} phenolic compounds. This transformation of benzyl phenyl ether into high carbon number phenolic compounds was less complex compared with the typical depolymerization and alkylation pathways.[9,10]

Our most significant finding was the simultaneous C–O breaking and C–C coupling of benzyl phenyl ether into high-carbon phenolics by metal triflates under a mild reaction condition (100 °C and 1 bar). Soluble catalysts such as metal triflates react efficiently with targeted linkages, minimize competing pathways, and enable the use of milder reaction conditions compared with solid catalysts.[24] Although investigators used Lewis acid salts as catalysts for the C–O cleavage of lignin model compounds, their focus was on the C–O cleavage into monomers. For example, Deuss *et al.*[25] and Shen *et al.*[26] used metal triflates to catalyze the C–O cleavage of the β-O-4 model compounds. However, only low-carbon number guaiacol-derived products (C_6–C_9) were produced. Similarly, Klein *et al.* used a combination of Pd/C and Lewis acid salts ($Zn(OAc)_2$,

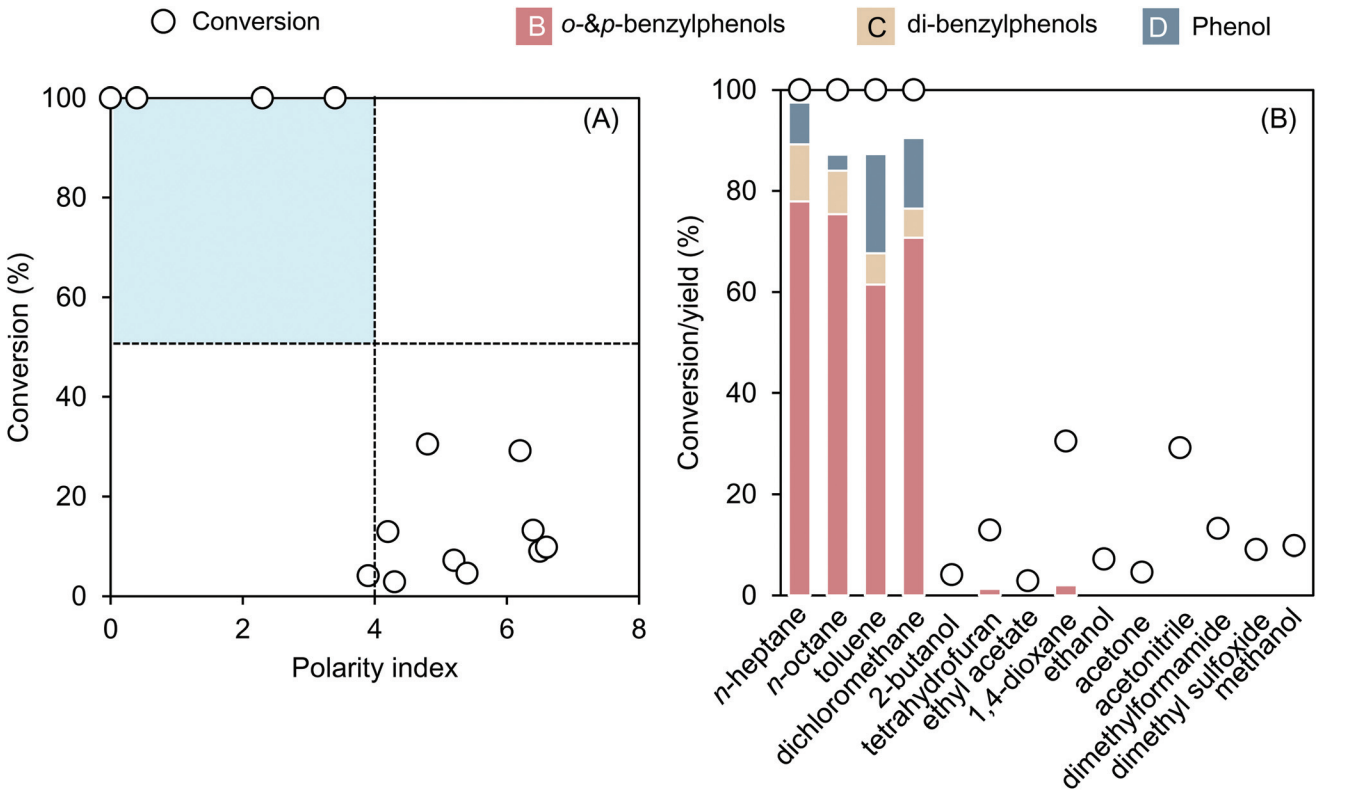

Fig. 4 Effect of solvents on the catalytic performance of hafnium triflate. (A) Conversion of benzyl phenyl ether as a function of the polarity index, and (B) feed conversion and product yield from reactions in various solvents. Reaction conditions: feed = 0.26 mmol benzyl phenyl ether, feed/solvent/dodecane (internal standard) = 1.0 : 8.5 : 0.5 by weight, $Hf(OTf)_4$ = 20 mol%, 100 °C, 1 bar, 1 h.

Published on 27 October 2021. Downloaded by University of Louisville on 11/18/2021 3:18:04 PM.

$FeCl_3$, $ZnCl_2$) as co-catalysts to cleave the β-O-4 model compounds in methanol and 35 bar H_2, which promoted the hydrogenolysis and hydrogenation into a mixture of phenolic monomers and their saturated analogs.[27] Huang *et al.* used a combination of metal triflates and Pd/C catalyst to cleave β-O-4, α-O-4, and 4-O-5 model compounds in methanol, 30 bar H_2 at 160–180 °C.[28] Although they used the α-O-4 model compound, they did not observe the C_{12}–C_{22} products because the presence of H_2 and hydrogen donor solvent (methanol) promoted hydrogenolysis and hydrogenation.

The classic acid-catalyzed depolymerization of compounds with aryl ether bonds focuses on the C–O cleavage and affords low yields of monomers because of condensation.[29] To be maximally useful, subsequent C–C coupling is needed to extend the carbon number of these compounds. The simultaneous C–O breaking and C–C coupling in our approach efficiently satisfies this requirement. Bai *et al.*[30] used Lewis acid sites of montmorillonite catalysts to promote the alkylation of phenol and benzyl acetate to produce benzylphenols at 140 °C. In addition, Bi *et al.*[10] and Zhang *et al.*[9] used a cascade of lignin depolymerization by HZSM-5 at 400–550 °C and alkylation by an acidic ionic liquid, $[C_4C_1im]Cl$–$2AlCl_3$, at 20–80 °C to produce C_8–C_{15} phenolics. Although high-carbon number phenolics were generated from these processes, the addition of an alkylation step requires additional catalysts and processing conditions that increase the production cost.[8] Instead, our process in which metal triflates catalyzed the direct C–O breaking and simultaneous C–C coupling of benzyl phenyl ether (α-O-4 bond) into two- and three-ring compounds eliminates any increased cost. In addition, our process suggested that the molecular structure of the ether bonds is important in product formation.

Significantly, the choice of the reaction solvent is important to maximize the catalytic performance of the transformation of benzyl phenyl ether. We found that low polar solvents with a polarity index less than 3.4 promoted catalyst activity and selectivity to desired products. Lin *et al.*[31] performed the Fries rearrangement of aryl esters over β-zeolite at 150 °C in solvents of polarities in the following order: *n*-decane < toluene < nitrobenzene < *N*-methyl-2-pyrrolidone < dimethylsulfoxide. They observed a decrease in the feed conversion as a function of increasing solvent polarity. Jayat *et al.*[32] applied β-zeolite for the Fries rearrangement of phenyl acetate in sulfolane and dodecane as a solvent at 160 °C. They found that the more polar sulfolane competed with phenyl acetate for adsorption on the acid sites, a result similar to our findings. Although the low-polar solvents enhanced the formation of our desired products (C_{12}–C_{22} phenolic compounds), high-polar solvents are preferred to solubilize the lignin-derived phenolics and enhance the contact between feed and catalysts. Moreover, these polar solvents, such as dioxane,[25] dimethylsulfoxide,[33] and alcohols[27,28] are typically used to fractionate and depolymerize lignin. Thus, additional studies should focus on the development of the active catalysts to produce C_{12}–C_{22} phenolic compounds in polar solvents. These C_{12}–C_{22} phenolic compounds (benzylphenols and di-benzylphenol products) have shown potential applications for phenolic-type polymers (phenol-formaldehyde resins),[34] diesel and jet fuel precursors,[7,8] and liquid organic hydrogen carriers.[35,36]

Although the C–O model compounds used in this study are commonly used to represent C–O bonds of lignin, they lack α and γ hydroxyl groups and methoxy group substitution patterns on the aromatic ring that mimic the combination of H, G, and S monomer units found in natural lignin. Moreover, previous studies showed that these functionalities affect chemical reactivity.[28,37,38] Studies in progress focus on the synthesis of α-O-4 model compounds with methoxy group substitution patterns on the aromatic ring and β-O-4 model compounds with α and γ hydroxyl groups and methoxy group substitution on the aromatic ring to determine the effect of these functionalities on the C–O breaking and C–C coupling.

Conclusion

Hafnium triflate catalyzed simultaneous C–O bond breaking and C–C bond coupling of benzyl phenyl ether into the large C_{12}–C_{22} phenolic compounds under a mild condition (100 °C and 1 bar). The conversion of benzyl phenyl ether and selectivity to the desired products increased with the decreasing polarity of solvents. Although we showed the potential of hafnium triflate to catalyze the direct C–O cleavage and C–C coupling of benzyl phenyl ether into C_{12}–C_{22} phenolics, a few questions remain. We are currently assessing the effect of methoxy group substitution patterns on the aromatic ring on the C–O breaking and C–C coupling of the α-O-4 model compounds; in addition, we are testing catalyst reuse and the ability to apply this chemical pathway to upgrade technical lignin.

Conflicts of interest

There are no conflicts to declare.

Acknowledgements

A portion of this material is based on work supported by the National Science Foundation under Cooperative Agreement No. 1355438. This work was performed in part at the Conn Center for Renewable Energy Research at the University of Louisville, which belongs to the National Science Foundation NNCI KY Manufacturing and Nano Integration Node, supported by ECCS-1542174. The authors would like to thank Dr. Howard Fried for his valuable comments and suggestions on the manuscript.

References

1 G. W. Huber and A. Corma, *Angew. Chem., Int. Ed.*, 2007, **46**, 7184–7201.

 This journal is © The Royal Society of Chemistry 2021

Published on 27 October 2021. Downloaded by University of Louisville on 11/18/2021 3:18:04 PM.

2 J. Ma, S. Shi, X. Jia, F. Xia, H. Ma, J. Gao and J. Xu, *J. Energy Chem.*, 2019, **36**, 74–86.
3 E. Adler, *Ind. Eng. Chem.*, 1957, **49**, 1377–1383.
4 S. Guadix-Montero and M. Sankar, *Top. Catal.*, 2018, **61**, 183–198.
5 P. C. Rodrigues Pinto, E. A. Borges da Silva and A. E. Rodrigues, *Ind. Eng. Chem. Res.*, 2011, **50**, 741–748.
6 W. Xu, S. J. Miller, P. K. Agrawal and C. W. Jones, *ChemSusChem*, 2012, **5**, 667–675.
7 J. Yoon, Y. Lee, J. Ryu, Y.-A. Kim, E. Park, J.-W. Choi, J.-M. Ha, D. Suh and H. Lee, *Appl. Catal., B*, 2013, **142**, 668–676.
8 H. Wang, H. Ruan, H. Pei, H. Wang, X. Chen, M. Tucker, J. Cort and B. Yang, *Green Chem.*, 2015, **17**, 5131–5135.
9 Y. Zhang, P. Bi, J. Wang, P. Jiang, X. Wu, H. Xue, J. Liu, X. Zhou and Q. Li, *Appl. Energy*, 2015, **150**, 128–137.
10 P. Bi, J. Wang, Y. Zhang, P. Jiang, X. Wu, J. Liu, H. Xue, T. Wang and Q. Li, *Bioresour. Technol.*, 2015, **183**, 10–17.
11 C. Zhao, D. M. Camaioni and J. A. Lercher, *J. Catal.*, 2012, **288**, 92–103.
12 C. Li, X. Zhao, A. Wang, G. W. Huber and T. Zhang, *Chem. Rev.*, 2015, **115**, 11559–11624.
13 K. Sanderson, *Nature*, 2011, **474**, S12–S14.
14 X. Cui, H. Yuan, K. Junge, C. Topf, M. Beller and F. Shi, *Green Chem.*, 2017, **19**, 305–310.
15 M. Frisch, G. Trucks, H. Schlegel, G. Scuseria, M. Robb, J. Cheeseman, G. Scalmani, V. Barone, B. Mennucci, G. Petersson, H. Nakatsuji, M. Caricato, X. Li, H. Hratchian, A. Izmaylov, J. Bloino, G. Zheng, J. Sonnenberg, M. Hada, M. Ehara, K. Toyota, R. Fukuda, J. Hasegawa, M. Ishida, T. Nakajima, Y. Honda, O. Kitao, H. Nakai, T. Vreven, J. Montgomery, J. Peralta, F. Ogliaro, M. Bearpark, J. Heyd, E. Brothers, K. Kudin, V. Staroverov, R. Kobayashi, J. Normand, K. Raghavachari, A. Rendell, J. Burant, S. Iyengar, J. Tomasi, M. Cossi, N. Rega, J. Millam, M. Klene, J. Knox, J. Cross, V. Bakken, C. Adamo, J. Jaramillo, R. Gomperts, R. Stratmann, O. Yazyev, A. Austin, R. Cammi, C. Pomelli, J. Ochterski, R. Martin, K. Morokuma, V. Zakrzewski, G. Voth, P. Salvador, J. Dannenberg, S. Dapprich, A. Daniels, Ö. Farkas, J. Foresman, J. Ortiz, J. Cioslowski and D. Fox, *Gaussian 09, Revision B. 01*, Gaussian, Inc., Wallingford, CT, 2009.
16 Y. Zhao and D. Truhlar, *Acc. Chem. Res.*, 2008, **41**, 157–167.
17 J. Tomasi, B. Mennucci and R. Cammi, *Chem. Rev.*, 2005, **105**, 2999–3094.
18 J. He, C. Zhao and J. A. Lercher, *J. Am. Chem. Soc.*, 2012, **134**, 20768–20775.
19 A. G. Sergeev and J. F. Hartwig, *Science*, 2011, **332**, 439–443.
20 L. Yang, Y. Li and P. Savage, *Ind. Eng. Chem. Res.*, 2014, **53**, 2633–2639.
21 R. Parthasarathi, R. A. Romero, A. Redondo and S. Gnanakaran, *J. Phys. Chem. Lett.*, 2011, **2**, 2660–2666.
22 A. Bagno, W. Kantlehner, R. Kreß and G. Saielli, *Z. Naturforsch., B: J. Chem. Sci.*, 2004, **59**, 386–397.
23 V. Roberts, S. Fendt, A. A. Lemonidou, X. Li and J. A. Lercher, *Appl. Catal., B*, 2010, **95**, 71–77.
24 P. Deuss, K. Barta and J. de Vries, *Catal. Sustainable Energy*, 2014, **4**, 1174–1196.
25 P. Deuss, C. Lahive, C. Lancefield, N. Westwood, P. Kamer, K. Barta and J. de Vries, *ChemSusChem*, 2016, **9**, 2974–2981.
26 X.-J. Shen, Q. Meng, Q. Mei, H. Liu, J. Yan, J. Song, D. Tan, B. Chen, Z. Zhang and G. Yang, *Chem. Sci.*, 2020, **11**, 1347–1352.
27 I. Klein, C. Marcum, H. Kenttämaa and M. M. Abu-Omar, *Green Chem.*, 2016, **18**, 2399–2405.
28 X. Huang, O. Gonzalez, J. Zhu, T. Korányi, M. Boot and E. Hensen, *Green Chem.*, 2017, **19**, 175–187.
29 E. Adler, *Wood Sci. Technol.*, 1977, **11**, 169–218.
30 J. Bai, Y. Zhang, X. Zhang, C. Wang and L. Ma, *ACS Sustainable Chem. Eng.*, 2021, **9**, 7112–7119.
31 R. Lin, S. Mitchell, T. Netscher, J. Medlock, R. Stemmler, W. Bonrath, U. Létinois and J. Pérez-Ramírez, *Catal. Sci. Technol.*, 2020, **10**, 4282–4292.
32 F. Jayat, M. Picot and M. Guisnet, *Catal. Lett.*, 1996, **41**, 181–187.
33 J. Mottweiler, T. Rinesch, C. Besson, J. Buendia and C. Bolm, *Green Chem.*, 2015, **17**, 5001–5008.
34 N. Dunga and N. Jumbam, *Macromol. Symp.*, 2012, **313**, 121–127.
35 P. Rao and M. Yoon, *Energies*, 2020, **13**, 6040.
36 X. Chen, C. Gierlich, S. Schötz, D. Blaumeiser, T. Bauer, J. Libuda and R. Palkovits, *ACS Sustainable Chem. Eng.*, 2021, **9**, 6561–6573.
37 C. Lahive, P. Kamer, C. Lancefield and P. Deuss, *ChemSusChem*, 2020, **13**, 4238.
38 M. A. Hossain, T. K. Phung, M. S. Rahaman, S. Tulaphol, J. B. Jasinski and N. Sathitsuksanoh, *Appl. Catal., A*, 2019, **582**, 117100.